Journal of Power Sources 243 (2013) 444–450

Contents lists available at SciVerse ScienceDirect

Journal of Power Sources

journal homepage: www.elsevier.com/locate/jpowsour

Ultrafast and stable hydrogen generation from sodium borohydride in methanol and water over Fe–B nanoparticles

Joey D. Ocon [a,b], Trinh Ngoc Tuan [a], Youngmi Yi [c], Rizalinda L. de Leon [b], Jae Kwang Lee [a], Jaeyoung Lee [a,*]

[a] Electrochemical Reaction and Technology Laboratory, School of Environmental Science and Engineering, Gwangju Institute of Science and Technology (GIST), Gwangju 500-712, Republic of Korea
[b] Department of Chemical Engineering, College of Engineering, University of the Philippines Diliman, Quezon City 1101, Philippines
[c] Fritz-Haber-Institut der Max-Planck-Gesellschaft, Faradayweg 4-6, Berlin D-14195, Germany

HIGHLIGHTS

- Optimized synthesis conditions for Fe–B nanoparticles with high hydrogen generation rates.
- Ultrafast and sustained H_2 generation rates in methanol solutions.
- Low activation energy values for $NaBH_4$ hydrolysis (64.26 kJ mol^{-1}) and methanolysis (7.02 kJ mol^{-1}) over Fe–B NPs.

GRAPHICAL ABSTRACT

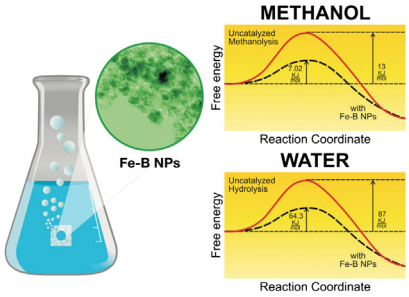

ARTICLE INFO

Article history:
Received 18 March 2013
Received in revised form
4 June 2013
Accepted 5 June 2013
Available online 13 June 2013

Keywords:
Hydrogen generation
Sodium borohydride
Iron boride nanoparticles
Methanolysis

ABSTRACT

Use of environmentally friendly hydrogen as fuel on a massive scale requires efficient storage and generation systems. Chemical hydrides, such as sodium borohydride ($NaBH_4$), have the capacity to meet these needs as demonstrated by its high hydrogen storage efficiency. Here, we first report the catalytic activity of Fe–B nanoparticles supported on porous Ni foam – synthesized *via* a simple chemical reduction technique – for hydrogen generation from the mixtures of $NaBH_4$, H_2O, and CH_3OH. Activation energies of the catalyzed hydrolysis (64.26 kJ mol^{-1}) and methanolysis (7.02 kJ mol^{-1}) are notably lower than other metal-boron catalysts previously reported. Methanol, in combination with a cheap but highly active Fe–B nanocatalysts, provides ultrafast rates of low temperature hydrogen generation from the sodium borohydride solutions.

© 2013 Elsevier B.V. All rights reserved.

1. Introduction

Fuel cells, such as a proton exchange membrane fuel cell (PEMFC), attract attention for a wide array of applications because they have high fuel efficiency, high power density, and zero emission. Portable PEMFC is a flexible and efficient way to meet the demand of electric power in urgency or in situations where cost is not a crucial factor [1]. In addition, the onboard storage and supply of hydrogen for PEMFC is an important barrier that needs to be overcome for the successful transition from energy based on fossil fuels to hydrogen-based systems. Borohydrides ($LiBH_4$, $NaBH_4$, KBH_4, etc.) are one of the most attractive materials for hydrogen storage due to their high volumetric and gravimetric hydrogen density, and they are safe to use [2]. Hydrogen gas is generated by

* Corresponding author. Tel.: +82 62 715 2440; fax: +82 62 715 2434.
E-mail address: jaeyoung@gist.ac.kr (J. Lee).

0378-7753/$ – see front matter © 2013 Elsevier B.V. All rights reserved.
http://dx.doi.org/10.1016/j.jpowsour.2013.06.019

the hydrolysis of borohydride in the presence of a suitable catalyst at room temperature according to the reaction below [3]:

$$NaBH_4 + 2H_2O \rightarrow 4H_2\uparrow + NaBO_2 \quad \left(\Delta H = -217\,kJ\,mol^{-1}\right) \qquad (1)$$

Some noble metals showed excellent catalytic activities in the hydrolysis of sodium borohydride, $NaBH_4$, solution to produce pure hydrogen [4–6]. Precious metal catalysts are expensive, while alloys and metals from nickel, cobalt, and iron are cheaper alternatives. Non-noble catalysts such as nickel- and cobalt-based have been explored previously [7–10]. Some initial studies on using non-optimized ferric catalysts, formed in situ during ferric salts infusion in $NaBH_4$ solution, exhibited promising results on the competing reactions during hydrogen evolution [11]. The catalytic activities of these alloys and metals are yet to be improved to be comparable with the noble metal catalysts.

One of the many challenges in the adoption of sodium borohydride H_2 storage system is the decrease in gravimetric efficiency associated with the hydration of the reaction by-products ($NaBO_2$) [1]. Furthermore, the alkaline by-products of sodium borohydride hydrolysis lower the reaction yield, which requires catalysts to accelerate the hydrolysis [12]. Light alcohols, such as methanol, are known to be reactive with sodium borohydride following Eq. (2). Although the extra weight from methanol relative to water decreases storage efficiency, methanol provides some attractive features such as reduced activation energy and possible reconversion of sodium tetramethoxyborate ($NaB(OCH_3)_4$) by-product to methanol (Eq. (3)) to increase storage and energy density of the system [13].

$$NaBH_4 + 4CH_3OH \rightarrow 4H_2\uparrow + NaB(OCH_3)_4 \qquad (2)$$

$$NaB(OCH_3)_4 + 2H_2O \rightarrow NaBO_2 + 4CH_3OH \qquad (3)$$

Although much is known about the kinetics of sodium borohydride in commonly studied catalysts, the hydrolysis and methanolysis of sodium borohydride in Fe–B catalyst has not received systematic study. In this study, we prepared Fe–B nanoparticles (Fe–B NPs) supported on nickel foam using a simple chemical reduction technique. The effects of catalyst loading, solution temperature, precursor, reducing, and stabilizer solution concentration on hydrogen generation rate were investigated to find the optimal conditions for catalyst synthesis.

2. Experimental

2.1. Catalyst synthesis

All the reagents were of analytical grade and used as received. The supported Fe–B catalysts were prepared by chemical reduction of an aqueous solution of iron chloride with a borohydride solution, as described in our previous works [8,10]. $FeCl_3$ (JUNSEI, Japan) and $NaBH_4$ (DAEJUNG, S. Korea) were used as iron precursor and reducing agent, respectively, while, sodium hydroxide served as a buffer agent. Reactant solutions were prepared at various concentrations: $FeCl_3$ (5.0–20.0 wt. %), $NaBH_4$ (5.0–20.0 wt. %), and NaOH (1.0–10.0 wt. %). The 1 cm^2 nickel foam (INCO-FOAM™) that was used as catalyst support is 2 mm thick and has 99.9% purity. The as-prepared catalysts were air-dried at 60 °C for 2 h. No further heat treatment at elevated temperatures was made since this was found to weaken the adhesion of the catalyst precipitate on the nickel foam support.

2.2. Catalyst characterization

Crystal structures of the catalyst were studied using X-ray diffraction (XRD, Rigaku D/MAXIIIA). The morphology and composition of the prepared catalysts were investigated by scanning electron microscopy (SEM, JEOL JSM 5200) and transmission electron microscopy (TEM, JEOL JEM-2100) equipped with X-ray energy dispersive spectrometer (EDS). The surface chemical properties of the FeB NPs were also examined by X-ray photoelectron spectroscopy (XPS, VG Multilab2000) with an Mg Kα X-ray source (1253.6 eV) at a base pressure of 2×10^{-9} Torr.

2.3. Hydrogen generation

To assess the catalytic activity, the synthesized catalysts were tested in a batch-type hydrogen generation system, consisting of a small glass reactor (PYREX, Japan) with an internal volume of 100 mL. As seen in the scheme in Fig. 1 for a typical measurement, the supported catalyst (1 cm^2) was introduced into the reactor along with the solution containing $NaBH_4$ and NaOH. The outgoing hydrogen stream was allowed to pass through a silica gel provision to remove moisture. Hydrogen generation rates (mL min^{-1}) were measured using a gas flow meter (Agilent ADM2000). The hydrogen generation rate was determined from the linear portion of the production rate time series. Catalyzed hydrogen production from $NaBH_4$ was also performed in water–methanol mixtures of different ratios. To evaluate the stability of the catalyst, the catalyst was reused over four cycles. After a catalytic hydrogen generation experiment, the catalyst was separated from the by-product solution, washed thoroughly with deionized water, and subsequently reused.

3. Results and discussion

3.1. Catalyst characterization

Fig. 2a shows a typical X-ray diffractogram of a representative precipitate collected at the surface of the Ni foam. During synthesis, the precipitate forms *via* the reduction reaction between the Fe^{3+} precursor solution and the $NaBH_4$ reducing solution. The XRD pattern is consistent with the pattern of polycrystalline Fe–B and $Fe(OH)_3$. Selected area electron diffraction (SAED) spots support the above observation, as shown by the multiple spotted ring patterns in Fig. 3d. EDS analysis confirmed that the principal components of the precipitate were boron, oxygen, and iron, as indicated in Fig. 2b and summarized in Table S1. Quantitative analysis revealed the atomic ratio of Fe and B to be 0.22, assuming all oxygen atoms present come from ferric hydroxide only.

The structure of the iron boride catalysts – sensitive to their synthesis condition – dictates the catalytic activity. As shown in the

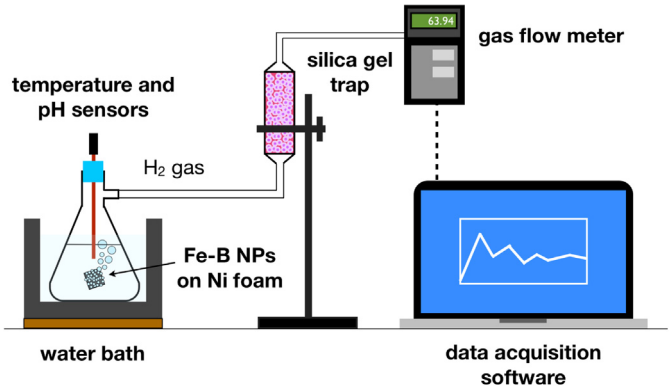

Fig. 1. Schematic illustration of the hydrogen generation set-up used to evaluate the catalytic activity of Fe–B NPs.

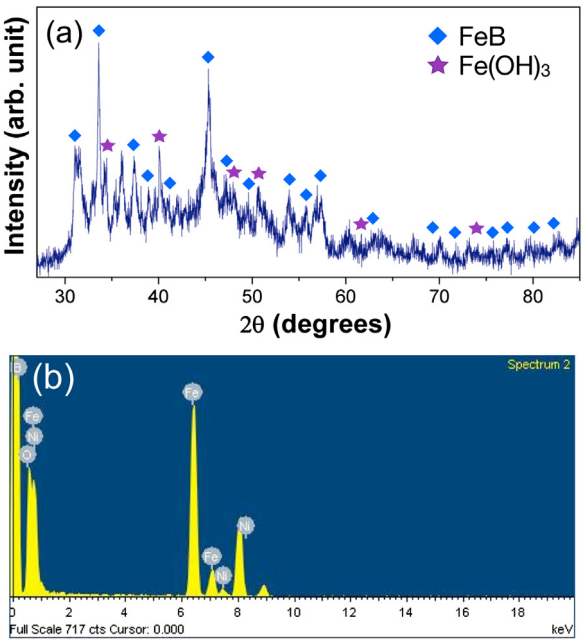

Fig. 2. (a) X-ray diffraction pattern and the (b) energy dispersive X-ray spectrum of a representative Fe–B catalyst. The catalyst was prepared by chemical reduction with the following condition: 15 dipping cycles, 15 wt. % $FeCl_3$, 15 wt. % $NaBH_4$, and 1 wt. % NaOH.

SEM image in Fig. 3a, the nanoparticles agglomerated into uniformly sized micro-scale aggregates. Furthermore, the size of the aggregates varies with precursor concentration, as seen in Fig. S1. Regardless of the precursor concentration, nanoparticles fully cover the support's surface. This indicates good contact between the support and catalyst particles that is needed to sustain high catalytic activity, especially during the vigorous initial phase in hydrogen generation. Examination in TEM (Fig. 3b) confirms the aggregation of catalyst particles. The Fe–B NPs have uniform sizes and their diameters range from 5 nm to 10 nm. Moreover, the HRTEM image displays the high degree of crystallinity of the orthorhombic Fe–B NPs, consistent with XRD results in Fig. 2a. Measurements on the lattice fringes of the nanocrystals (Fig. 3c) were in excellent agreement with the dimensions of orthorhombic Fe–B. When the effect of synthesis condition was considered, we found that it has no effect on the particle size and crystallinity of Fe–B NPs, however, a significantly higher degree of influence was found to the catalyst loading on the support as discussed in the succeeding section.

3.2. Optimization of catalyst preparation

In order to improve the rate of hydrogen generation from sodium borohydride hydrolysis, we studied the effect of each variable during the preparation of the catalyst. The main variables considered were the number of dip-coating cycles, precursor concentration ($FeCl_3$), reductant concentration ($NaBH_4$) and stabilizer concentration (NaOH). Fig. 4a shows the effect of dip-coating frequency on the catalyst loading and hydrogen generation. As seen in the figure, amount of Fe–B deposited on the Ni substrate increased linearly with number of dip-coating cycles. Expectedly, hydrogen generation rates rose with the amount of catalyst. High catalyst loading and generation efficiency observed at fifteen dip-coating cycles were the reasons why subsequent experiments used fifteen dipping cycles.

Supported catalysts were also prepared using different precursor solution concentrations (5.0, 10.0, 15.0, and 20.0 wt. %). We found that the precipitate's color shifted from brown to black as the

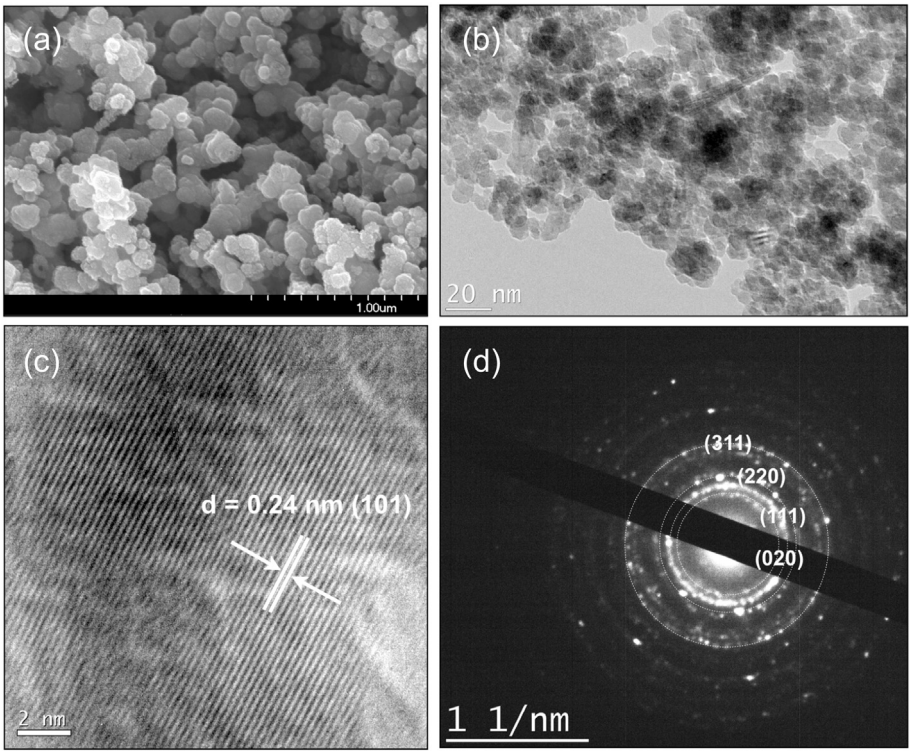

Fig. 3. (a) SEM, (b) TEM, and (c) high resolution TEM (HRTEM) images of a representative Fe–B catalyst, and the corresponding (d) selected area electron diffraction pattern. The catalyst was prepared by chemical reduction with the following condition: 15 dipping cycles, 15 wt. % $FeCl_3$, 15 wt. % $NaBH_4$, and 1 wt. % NaOH.

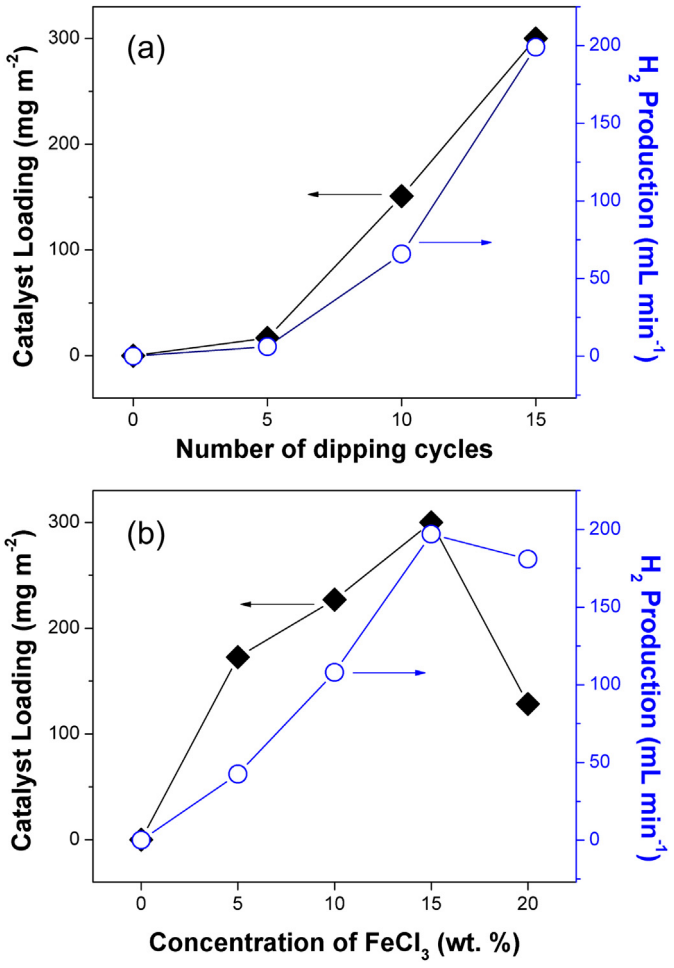

Fig. 4. (a) Effect of the number of dip-coating cycles on the catalyst loading on Ni foam and H_2 generation (synthesis condition: 15.0 wt. % $FeCl_3$, 15.0 wt. % $NaBH_4$ and 1.0 wt. % NaOH) (b) effect of the precursor solution, $FeCl_3$, concentration on the catalyst loading and H_2 generation: (synthesis condition: 15 dipping cycles, 10.0 wt. % $NaBH_4$, and 1.0 wt. % NaOH).

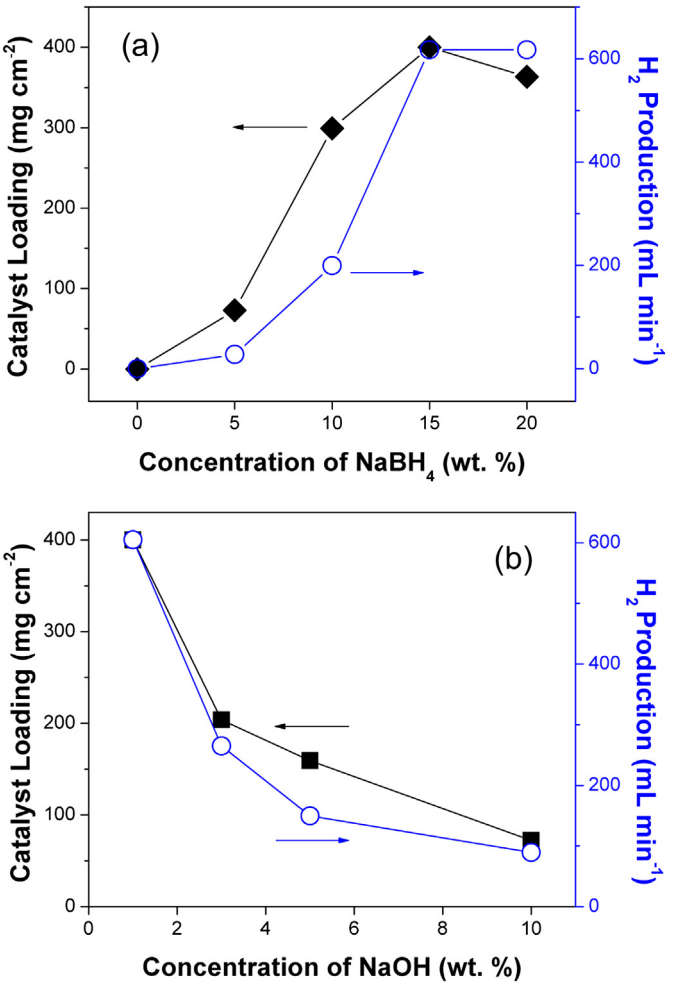

Fig. 5. (a) Effect of the reducing solution, $NaBH_4$, concentration on the catalyst loading and H_2 generation: (synthesis condition: 15 dipping cycles, 15.0 wt. % $FeCl_3$, and 1.0 wt. % NaOH) (b) effect of the stabilizer, NaOH, concentration on the catalyst loading and H_2 generation: (synthesis condition: 15 dipping cycles, 15.0 wt. % $FeCl_3$, and 10.0 wt. % $NaBH_4$).

concentration of the precursor solution increased. This indicates that more Fe–B catalysts are formed on the substrate, in good agreement with the observations in Ref. [11]. As seen in Fig. 4b, the amount of Fe–B NPs surged considerably with the concentration of the precursor solution. The weight of the catalysts loaded for 5.0, 10.0, 15.0, and 20.0 wt. % $FeCl_3$ are 170 mg cm^{-2}, 225 mg cm^{-2}, 300 mg cm^{-2}, and 128 mg cm^{-2}, respectively. While the loading rose up to 15 wt. % $FeCl_3$, the reduction reaction at 20 wt. % $FeCl_3$ occurred strongly and uncontrollably, which decreased the catalyst loading and hydrogen generation rate.

We found a similar tendency for catalysts fabricated at different reductant concentrations. As shown in Fig. 5a, the amount of Fe–B catalyst coated on the support rose linearly with increasing $NaBH_4$ concentration (5.0, 10.0 and 15.0 wt. %) with values of 72.9, 300.0, and 399.1 mg cm^{-2}, respectively; but decreased to 362.5 mg cm^{-2} at 20.0 wt. % $NaBH_4$. It was observed that at a very high concentration of $NaBH_4$, the reduction reaction was also strong and non-controllable and it caused difficulty for Fe–B catalyst to adsorb well on nickel foam. Meanwhile, increasing $NaBH_4$ concentration in the reducing solution boosted the hydrogen production rate. From a concentration of 5.0 to 10.0 wt. %, hydrogen generation rate ascended slowly, from 28.7 to 198.0 mL min^{-1} and at $NaBH_4$ concentrations of 15.0 and 20.0 wt%, the rates rose steeply to 617 and 618 mL min^{-1}. Hence, high generation rates suggest that the reduction reaction was dominated by Fe–B formation at 15.0 wt. % $FeCl_3$, with most of the Fe^{3+} reduced by BH_4^- to form the Fe–B NPs.

The reduction reaction of metal salt with $NaBH_4$ and hydrolysis of $NaBH_4$ to generate hydrogen are usually conducted in a base-stabilized condition to avoid self-hydrolysis. The effect of NaOH concentration on catalyst preparation and hydrogen generation rate is shown in Fig. 5b. Our findings demonstrate that the increase in the amount of NaOH stabilizer exerted a negative effect on the amount of catalyst loaded on nickel foam and correspondingly the hydrogen generation rate. As the NaOH concentration rose from 1.0 to 10.0 wt. %, the amount of catalysts loaded on nickel foam decreased from 399.1 to 70.3 mg cm^{-2} and the hydrogen generation rate declined from 617 to 133 mL min^{-1}. We can attribute this decrease in generation rate from the inhibiting effect of hydroxide ions. First, hydroxide ions react with water thereby decreasing the free water available for $NaBH_4$ hydrolysis to produce hydrogen. Second, higher concentration of hydroxide ions forms more of the passive $Fe(OH)_3$ precipitate. To further prove this point, hydrogen generation rates of sodium borohydride decreased at higher NaOH concentrations, while, the precipitate color changed from black to brown.

Using these results, we synthesized nickel-supported Fe–B NPs *via* the conditions that showed superior activity and investigated

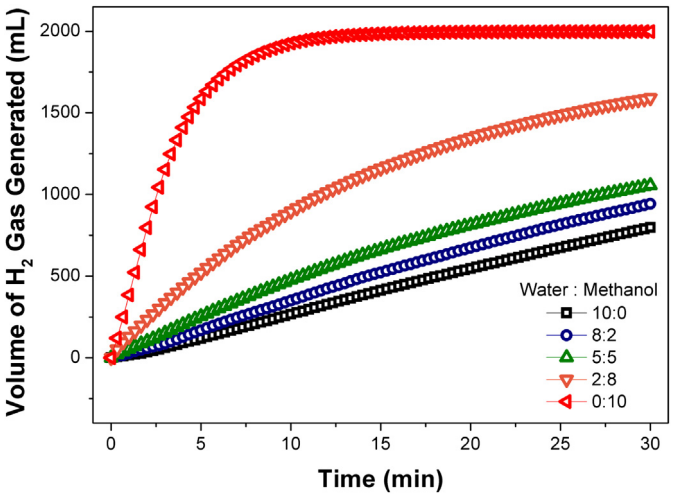

Fig. 6. Total hydrogen production (mL) from 1.0 g of sodium borohydride in 100 mL of various water–methanol mixtures over Fe–B NPs. The catalyst was prepared by chemical reduction with the following optimized condition: 15 dipping cycles, 15 wt. % $FeCl_3$, 15 wt. % $NaBH_4$, and 1 wt. % NaOH.

$NaBH_4$ hydrolysis at different reactor temperature levels (20.0, 30.0, 40.0 and 50.0 in °C). Hydrogen generation rates surged dramatically with reactor temperature, following the Arrhenius equation. As the solution temperature was elevated from 20 to 50 °C, steady-state hydrogen generation rates increased from 461 to 5487 mL min^{-1} g^{-1}. As computed from the Arrhenius plot in Fig. S2, activation energy is 64.26 kJ mol^{-1} with a correlation factor (R^2) of 0.97. This result compares well to previously reported kinetics of non-noble hydrolysis catalysts.

Judging from the results above, Fe–B NPs display superior catalytic activity for hydrogen generation from sodium borohydride solutions. Although, it is difficult to give definitive reasons as to why the FeNPs show lower activation energy without *ab initio* molecular dynamics simulations, we can surmise that this is due to the nanoparticle size effects. The nanoscale Fe–B catalyst, undoubtedly, has enhanced catalytic activity that might be due to higher surface area, better porous structure, or a more diverse energy level spectrum in its electronic structure – factors that favor faster reaction kinetics [14].

3.3. Hydrogen generation in methanol and water

To test the effect of using methanol as $NaBH_4$ solvent, rates of hydrogen generation for converting one gram of $NaBH_4$ in solutions at different water–methanol ratios were measured. These experiments were conducted in the absence of a stabilizer but in the presence of the nanocatalysts prepared using the optimized condition. Hydrogen generation rates increased with higher methanol concentration, as presented by the total hydrogen volume collected with time in Fig. 6. As shown in the figure, the fastest turnover rate was observed for pure methanol, consistent with the observations for the self-methanolysis of $NaBH_4$ in Ref. [13], but at a relatively faster rate due to the presence of the catalyst. Significantly higher initial rates were recorded, as indicated by the steeper slopes of the tangents at the initiation of the reaction, as the higher the methanol concentration in the solvent. Even if there was an increase in pH during the reaction – since high pH decreases generation rate – almost 90% of the hydrogen present in the borohydride was delivered in the first five minutes of the reaction in pure methanol. This is important for applications needing ultrafast low temperature generation of hydrogen from sodium borohydride.

In order to study the possible changes in the surface specie before and after hydrogen generation, XPS analysis was performed. Three major conditions were studied: pristine Fe–B, the Fe–B catalyst after H_2 generation in $NaBH_4$ solutions (water, methanol, and 1:1 water–methanol mixture), and a regenerated methanolysis catalyst. During regeneration, a catalyst used in methanolysis was immersed in deionized water for 5 min. As shown in Fig. 7a, the Fe2p spectra remained almost unchanged before and after hydrogen generation in water, methanol, and water–methanol mixture solutions. This represents excellent chemical stability of the Fe–B particles in different operating conditions.

Quantification of the Fe2p XPS spectra revealed that the atomic percentage of Fe in the pristine Fe–B NPs is 14.67 at. %. Upon H_2 generation in the three $NaBH_4$ solutions, it decreased to 7.57 at. %, 7.03 at. %, and 4.51 at. %, corresponding to $NaBH_4$ solutions in water, methanol, and water–methanol mixture, respectively. It is believed that the decrease in the at. % of Fe in the catalyst's surface is due to the formation and accumulation of reaction by-products at the surface. Qualitative examination of the Fe2p XPS spectrum in the regenerated catalyst showed an at. % almost the same as the pristine catalyst (14.79 at. %). The additional set of spectra for Na1s and C1s provided the same results about the catalyst regeneration. As shown in Fig. 7b, the Na1s XPS peak after methanolysis, which

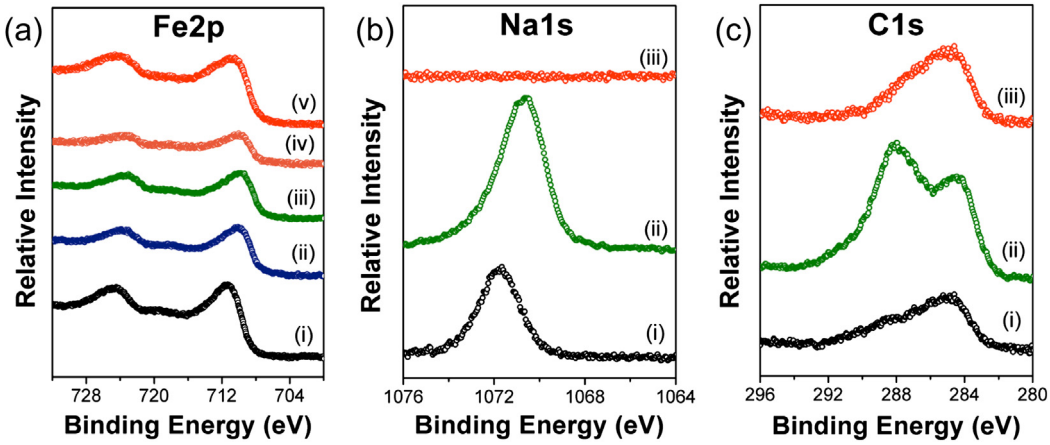

Fig. 7. (a) Fe2p XPS spectra of the catalyst at different conditions: (i) as-prepared Fe–B NPs, (ii) after hydrolysis, (iii) after methanolysis, (iv) after H_2 generation in 1:1 water–methanol mixture, and (v) after catalyst regeneration, (b) Na1s XPS spectra of the catalyst at different conditions: (i) as-prepared Fe–B NPs, (ii) after methanolysis, and (iii) after catalyst regeneration, and (c) C1s spectra XPS spectra of the catalyst at different conditions: (i) as-prepared Fe–B NPs, (ii) after methanolysis, and (iii) after catalyst regeneration.

correspond to the $NaB(OCH_3)_4$ product, disappeared after regeneration. Moreover, the C1s XPS spectrum of the regenerated catalyst exhibited similar peaks with that in the pristine catalyst (Fig. 7c). The strong C1s peak at higher binding energy (~288 eV) formed after methanolysis vanished after regeneration. The reconversion of the sodium tetramethoxyborate by-product, as seen in the XPS results, is in agreement with the X-ray diffraction, FT-IR, and Energy-dispersive X-ray spectroscopy results of two other studies [13,21].

The effect of sodium borohydride concentration on the hydrogen production reaction rate for pure methanol and pure water, in the absence of NaOH, was studied. The hydrogen generation volume was observed to increase for all $NaBH_4$ concentrations, as seen in Fig. 8. We found that the generation rate rose with $NaBH_4$ concentration for both cases. This result is similar with that reported for ruthenium catalysts [5]. They found that generation rates went up from low concentrations to until 10.0 wt. % and decreased beyond it. The decrease in generation rate at higher concentrations was attributed to the higher viscosity and possibly resulting from mass diffusion limitations. Viscosity effects on the reaction rate from Na^+ and BH_4^- ions are assumed to be insignificant here since relatively small amounts (less than 1.0 wt. %) of $NaBH_4$ were used. Using an *ln–ln* plot of the hydrogen generation rate *vs.* sodium borohydride concentration, we found that the reaction in pure methanol is pseudo-first order with respect to sodium borohydride concentration. It is possible to confirm that in the presence of methanol with no added

Table 1
Activation energy compiled from various kinetic studies of hydrogen generation from $NaBH_4$.

Catalyst	Temperature (°C)	Activation energy (kJ mol^{-1})	References
Pt/C	25	45.0	[16]
Ru/resin	25–55	47.0	[17]
Co powder	22	75.0	[18]
Ni cluster	25–45	54.0	[19]
Ni–Co–B	8–27	62.0	[20]
Pure methanol (no catalyst)	5–55	13.0	[13]
Fe–B NPs (in water)	20–50	64.26	Present study
Fe–B NPs (in methanol)	20–50	7.02	Present study

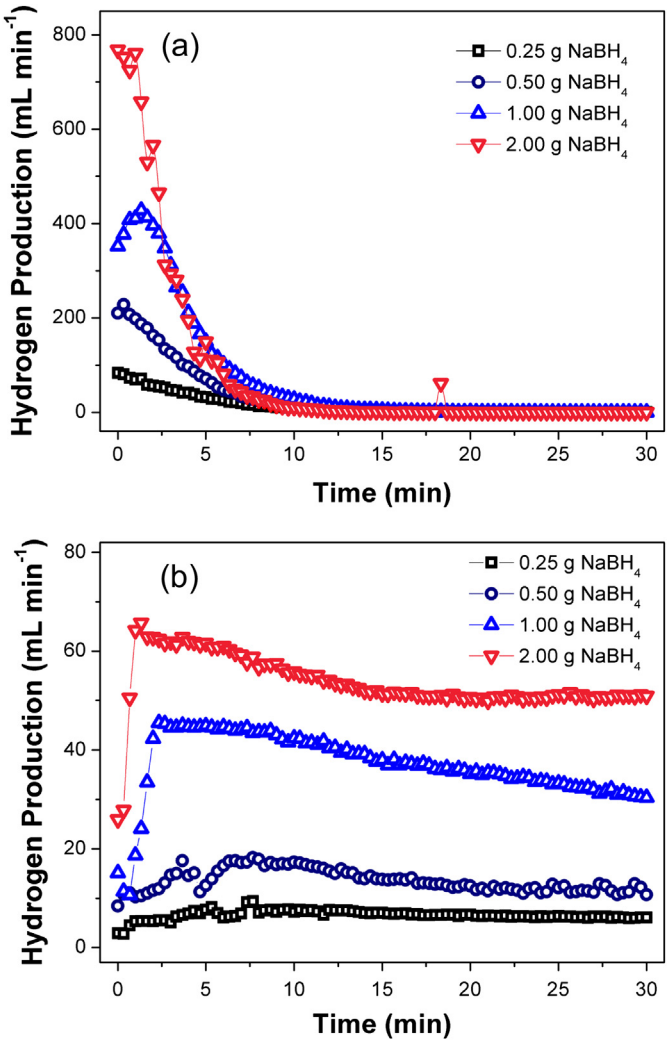

Fig. 8. Effect of amount of $NaBH_4$ in hydrogen generation in (a) pure methanol and in (b) pure water. The catalyst was prepared by chemical reduction with the following optimized conditions: 15 dipping cycles, 15 wt. % $FeCl_3$, 15 wt. % $NaBH_4$, and 1 wt. % NaOH.

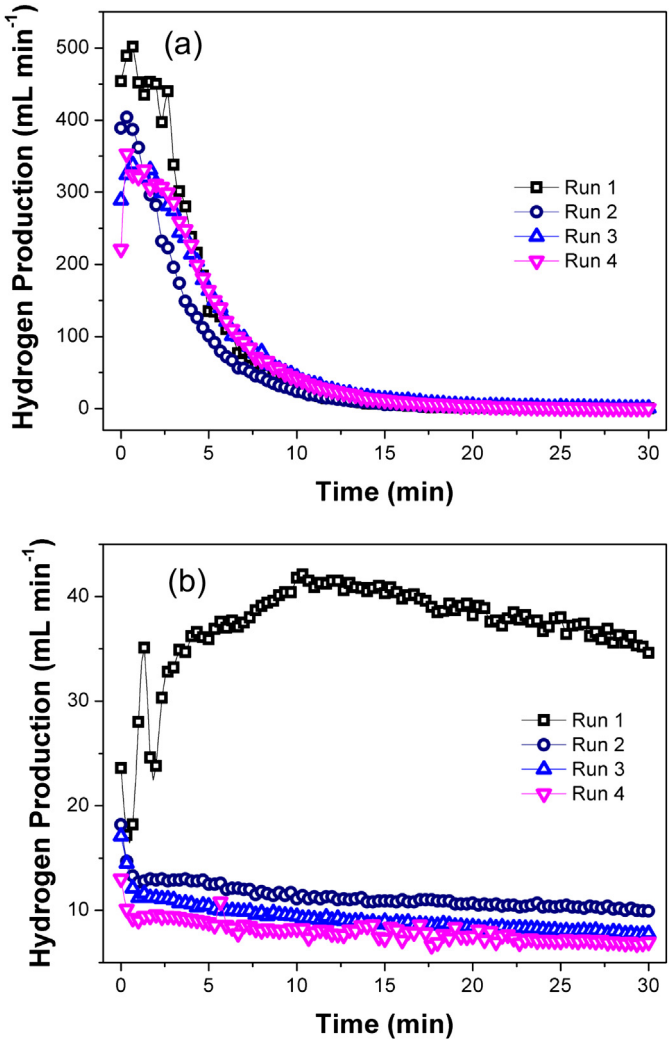

Fig. 9. Four successive hydrogen generation runs using the same catalyst in (a) pure methanol and (b) in pure water. Generation rates of the Fe–B NPs were more stable in methanol than in water due to less formation of solid by-products that can block the active sites.

water, the conversion rate of $NaBH_4$ is higher than the self-hydrolysis and self-methanolysis [12,15].

The $NaBH_4$ reaction kinetics in methanol, over Fe–B NPs, was further investigated at different temperatures. The hydrogen generation rate profiles at various temperatures in the range of 20–50 °C were taken. An Arrhenius plot was constructed where the logarithmic of the hydrogen generation rate was plotted against the reciprocal of absolute temperature ($1/T$), as shown in Fig. S3. The activation energy was calculated to be 7.02 kJ mol^{-1} (R^2 of 0.95) for the Fe–B NP-catalyzed methanolysis of sodium borohydride. This value is significantly lower than other activation energies in literature. Experimental results from various studies are shown here for comparison, *see* Table 1. The exceptionally low activation energy showed essentially that ultrafast generation of hydrogen is possible when using methanol as solvent. Although, pure methanol as solvent considerably lowers the gravimetric capacity, methanol–water mixtures can be employed instead, in complement with the use of a non-noble metal catalyst.

Finally, cycle tests were performed to investigate the stability and durability of the Fe–B NPs on nickel foam. Here, we used the same catalyst for four successive runs and gathered the generation rate profiles for both water and methanol. Fig. 9 shows the generation rates for the four successive runs in methanol and water. The decrease in catalyst performance in water might be caused by the formation of reaction by-products, $NaBO_2$, at the catalyst surface leading to catalyst deactivation. As seen in the XPS results, reaction by-products form and accumulate on the catalyst' surface during hydrogen production. Yet, there was minimal decrease in activity in methanol solutions, as shown in Fig. 8a. This suggests that aside from accelerating the reaction rates, generating hydrogen in methanol solutions can lead to a more stable and reliable production of hydrogen.

4. Conclusion

In this work, we explore the catalytic activity of Fe–B NPs, reported here for the first time, for hydrogen generation from sodium borohydride. Our results demonstrate that the activity depends on several key factors: number of dip-coating cycles, $FeCl_3$ concentration, $NaBH_4$ concentration, and NaOH concentration. Furthermore, activation energies of catalyzed hydrolysis and methanolysis are 64.26 kJ mol^{-1} and 7.02 kJ mol^{-1}, respectively, and these are comparable with most published data on noble metal and other metal-boron catalysts. We have further verified that methanol can be recovered from the methanolysis by-product after catalyst regeneration in water. Hence, any system where hydrogen is generated from sodium borohydride in water–methanol mixtures can be described as heterogeneously (Fe–B NPs) and homogeneously (methanol) catalyzed. Although methanol lowers the gravimetric capacity, the use of methanol as an additive to water simultaneously with a non-noble catalyst, i.e. Fe–B NPs, can enhance and stabilize the hydrogen generation rate. This is especially useful for fuel cell applications needing ultrafast hydrogen generation rates during start-up and operation. For practical application, we envision a continuous H_2 generation system where water and sodium borohydride are constantly replenished in the reactor that is equipped with cheap and non-noble metal-boron catalysts. While an optimal amount of methanol is needed to accelerate the production rate, it should not be too high that it drastically lowers the gravimetric capacity.

Acknowledgment

This work was supported by the National Research Foundation (NRF) grant funded by the Korean Government (MEST) (2010-0022453). J.D. Ocon gratefully acknowledges the DOST-UP ERDT Faculty Development Program.

Appendix A. Supplementary data

Supplementary data related to this article can be found at http://dx.doi.org/10.1016/j.jpowsour.2013.06.019.

References

[1] H. Senoh, Z. Siroma, N. Fujiwara, K. Yasuda, J. Power Sources 185 (2008) 1.
[2] H.C. Brown, C.A. Brown, J. Am. Chem. Soc. 84 (1962) 1493.
[3] H.I. Schlesinger, H.C. Brown, A.E. Finholt, J.R. Gilbreath, H.R. Hoekstra, E.K. Hyde, J. Am. Chem. Soc. 75 (1953) 215.
[4] C. Wu, H. Zhang, B. Yi, Catal. Today 93 (2004) 477.
[5] S.C. Amendola, S.L. Sharp-Goldman, M.S. Janjua, N.C. Spencer, M.T. Kelly, P.J. Petillo, M. Binder, Int. J. Hydrogen Energy 25 (2000) 969.
[6] Y. Kojima, K. Suzuki, K. Fukumoto, M. Sasaki, T. Yamamoto, Y. Kawai, H. Hayashi, Int. J. Hydrogen Energy 27 (2002) 1029.
[7] C. Wu, F. Wu, Y. Bai, B. Yi, H. Zhang, Mater. Lett. 59 (2005) 1748.
[8] J. Lee, K.Y. Kong, C.R. Jung, E. Cho, S.P. Yoon, J. Han, T.G. Lee, S.W. Nam, Catal. Today 120 (2007) 305.
[9] D. Hua, Y. Hanxi, A. Xinping, C. Chuansin, Int. J. Hydrogen Energy 28 (2003) 1095.
[10] J.K. Lee, H. Ann, Y. Yi, K.W. Lee, S. Uhm, J. Lee, Catal. Commun. 16 (2011) 120.
[11] C. Wu, Y. Bai, F. Wu, Mater. Lett. 62 (2008) 4242.
[12] E.Y. Marrero-Alfonso, J.R. Gray, T.A. Davis, M.A. Matthews, Int. J. Hydrogen Energy 32 (2007) 4723.
[13] V.R. Fernandes, A.M.F.R. Pinto, C.M. Rangel, Int. J. Hydrogen Energy 35 (2010) 9862.
[14] P. Hervés, M. Pérez-Lorenzo, L.M. Liz-Marzán, J. Dzubiella, Y. Lu, M. Ballauff, Chem. Soc. Rev. 41 (2012) 5577.
[15] C.F. Lo, K. Karan, B.R. Davis, Ind. Eng. Chem. Res. 46 (2007) 5478.
[16] G. Guella, B. Patton, A. Miotello, J. Phys. Chem. C 111 (2007) 18744.
[17] S.C. Amendola, S.L. Sharp-Goldman, M.S. Janjua, M.T. Kelly, P.J. Petillo, M. Binder, J. Power Sources 85 (2000) 186.
[18] C.M. Kaufman, B. Sen, J. Chem. Soc. Dalton Trans. 2 (1985) 307.
[19] Ö. Metin, S. Özkar, Int. J. Hydrogen Energy 32 (2007) 1707.
[20] J.C. Ingersoll, N. Mani, J.C. Thenmozhiyal, A. Muthaiah, J. Power Sources 173 (2007) 450.
[21] D. Xu, L. Zhao, P. Dai, S. Ji, J. Nat. Gas Chem. 21 (2012) 488.